Supplementary Information (SI) for Journal of Materials Chemistry B.

Supporting Information

Enhanced catalytic efficiency of nanozyme with V-structured chip for microfluidic biosensing of *S. typhimurium*

Ming-Yue Gao, Meng Wang, Yong-Tao Wang and Zhi-Ling Zhang*

College of Chemistry and Molecular Sciences, Wuhan University, Wuhan, 430072, China.

*E-mail: zlzhang@whu.edu.cn

Content

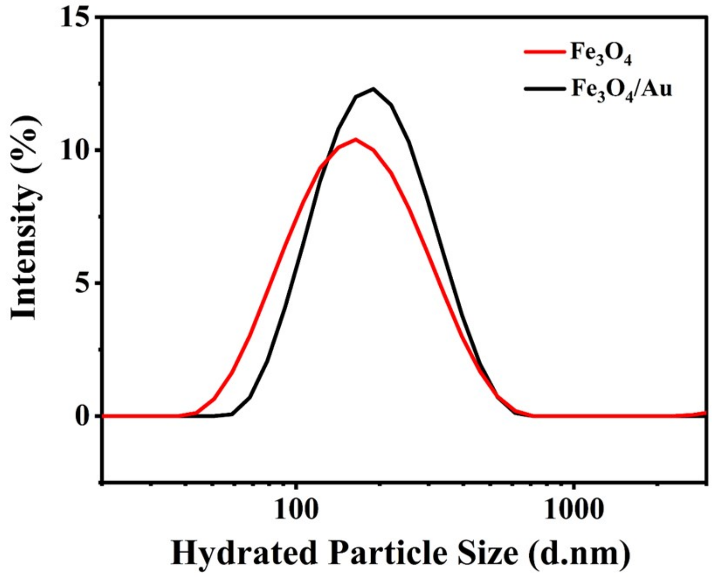

Fig. S1 Hydrated particle size distribution of Fe_3O_4 NPs and Fe_3O_4/Au NPs measured by DLS.

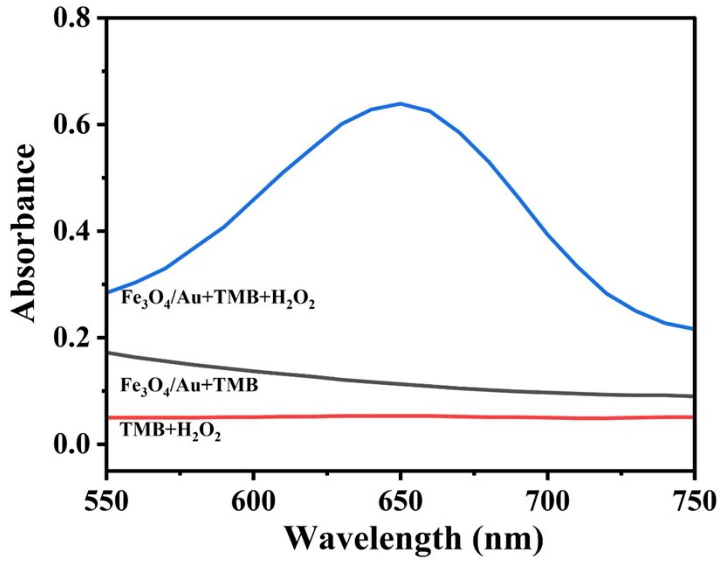

Fig. S2 UV−vis absorption spectra for the peroxidase-like catalytic activity of different reaction systems.

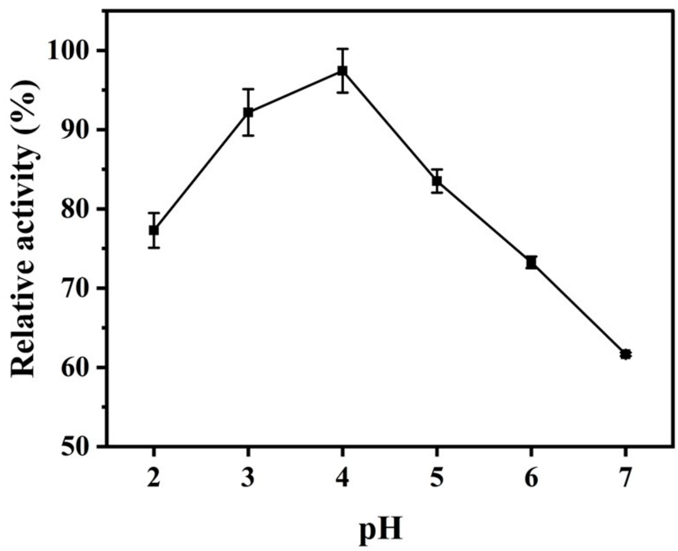

Fig. S3 Effect of pH on the peroxidase-like catalytic activity of Fe_3O_4/Au NPs.

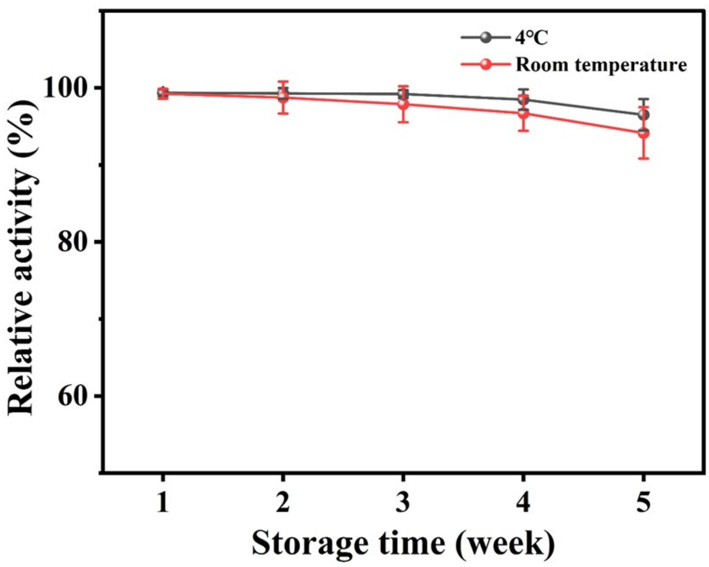

Fig. S4 Effect of storage time on the peroxidase-like catalytic activity of Fe_3O_4/Au NPs.

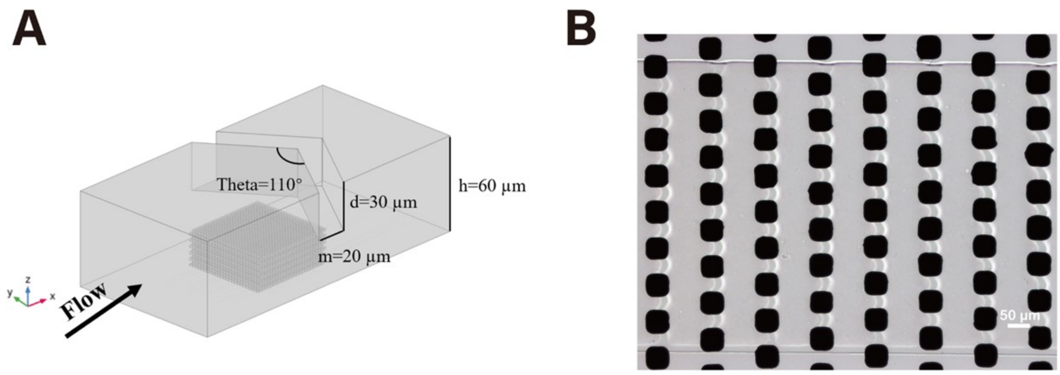

Fig. S5 (A) Optimized parameters and (B) microscopic image of the V-structure.

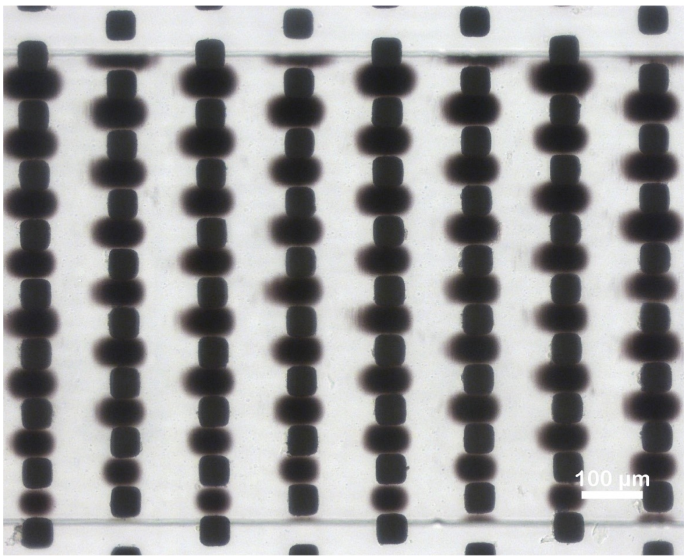

Fig. S6 Microscopic image of the magnetic nanozyme array consisted of Fe_3O_4/Au NPs.

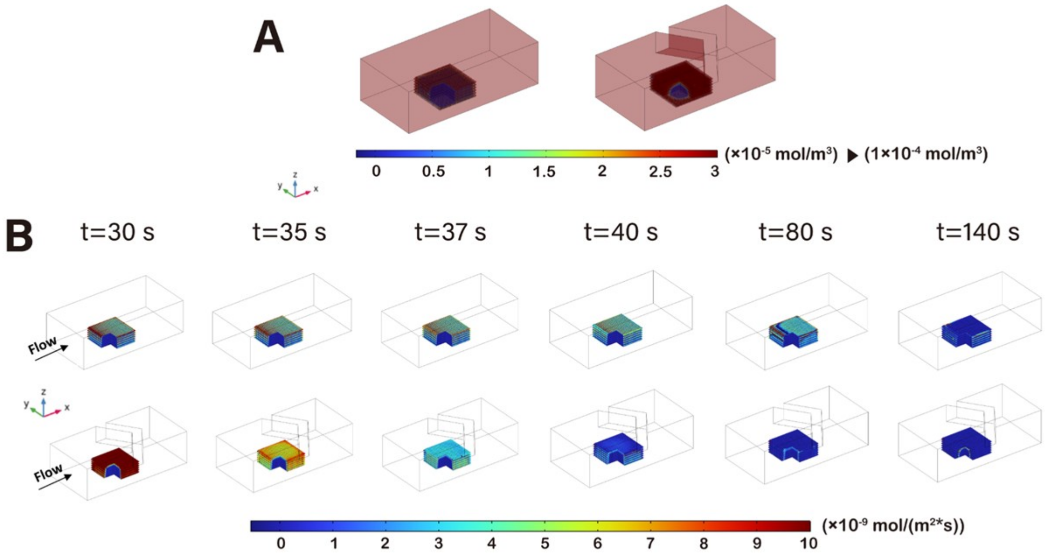

Fig. S7 (A) Simulation of the substrate concentration field distribution. t=200 s. (B) Simulation of the binding reaction rate at different time points.

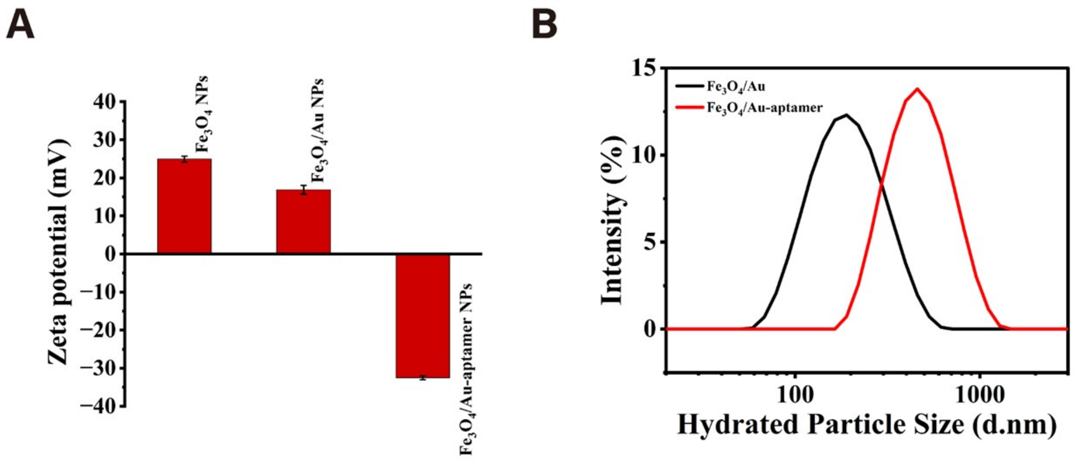

Fig. S8 (A) Zeta potential of Fe_3O_4 NPs, Fe_3O_4/Au NPs, and Fe_3O_4/Au-aptamer NPs. (B) Hydrated particle size of Fe_3O_4/Au NPs and Fe_3O_4/Au-aptamer NPs.

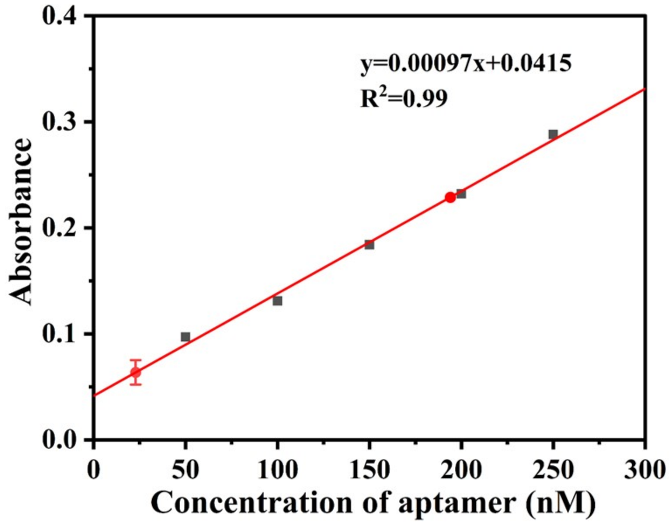

Fig. S9 Measurement of the amount of DNA aptamer per milligram Fe_3O_4/Au NPs. Red line: the calibration curve of DNA aptamer concentration based on absorbance at 260 nm. Red points: the concentration of DNA aptamer before and after the conjugation (N=3).

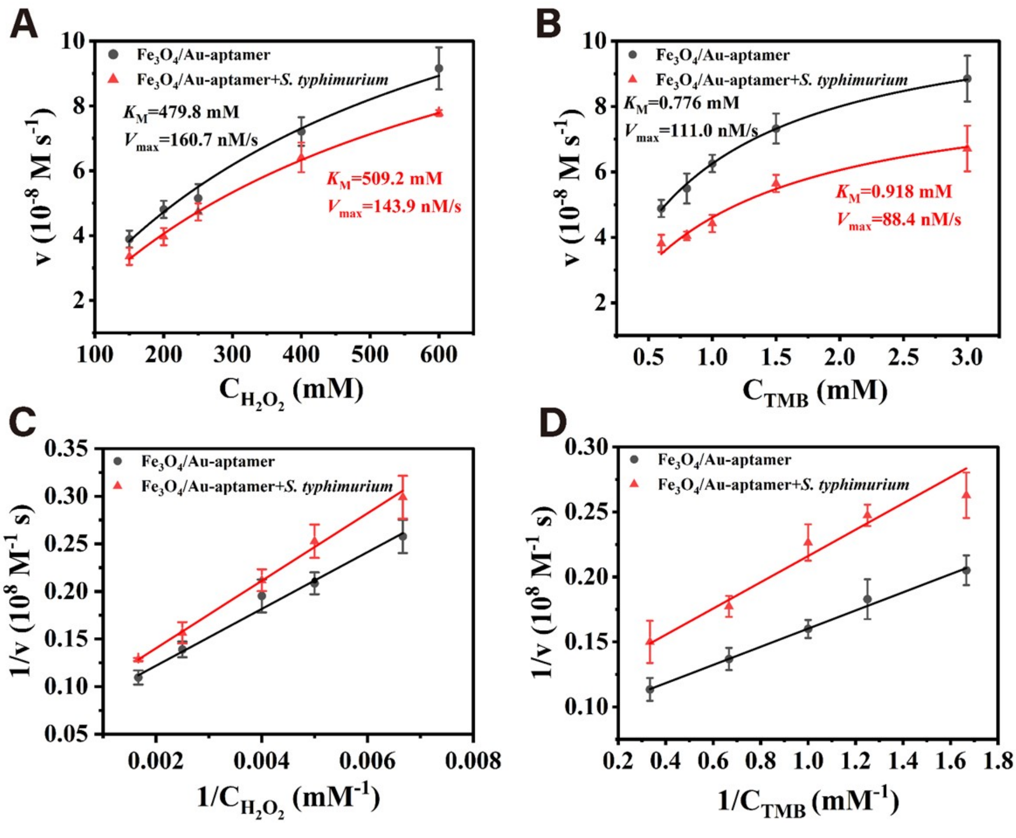

Fig. S10 Steady state kinetic study of Fe_3O_4/Au-aptamer NPs in the presence and absence of *S. typhimurium* with the concentration of TMB (A) and H_2O_2 (B) fixed at 525 µM and 200 mM, respectively. Double reciprocal plots of catalytic activity of Fe_3O_4/Au-aptamer NPs in the presence and absence of *S. typhimurium* with the concentration of TMB (C) and H_2O_2 (D) fixed at 525 µM and 200 mM, respectively.

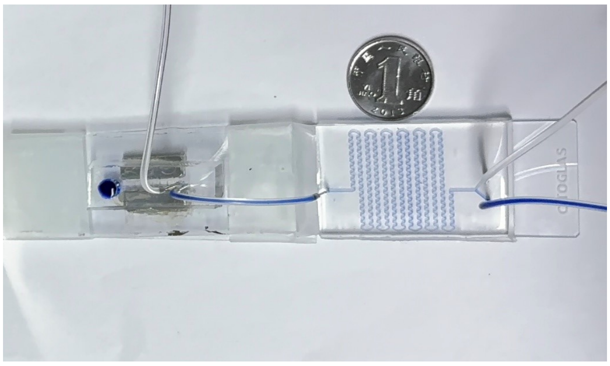

Fig. S11 Photo of the integrated microfluidic chip.

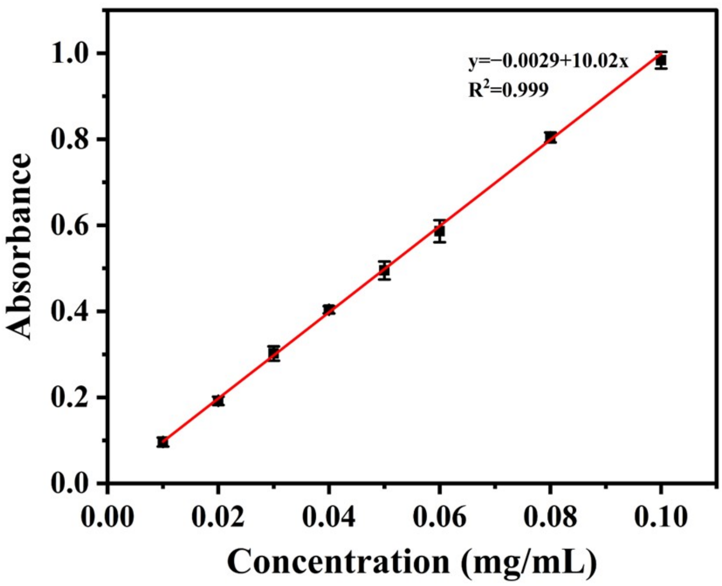

Fig. S12 Absorbance of Fe_3O_4/Au NPs at 550 nm at different concentrations.

Table S1 Comparison with the reported detection methods of *S. typhimurium*.

Methods	Instruments	LOD (CFU/mL)	Linear range (CFU/mL)	Time	References
Fluorescence	Microplate reader	4	10^1-10^6	2.5 h	1
Fluorescence	Microplate reader	150	6.2×10^2-6.2×10^6	3.5 h	2
Thermal imaging	Smartphone	93	1.01×10^2-1.01×10^6	<1 h	3
Electrochemical	Electrochemical station	55	6.7×10^1-6.7×10^5	<2.5 h	4
Surface-enhanced Raman scattering	Hand-held Raman spectrometer	3	10^0-10^8	45 min	5
Colorimetric	UV-vis spectrophotometer	0.51	1.93×10^1-1.93×10^5	40 min	6
Colorimetric	Smartphone	44	4.4×10^1-4.4×10^6	45 min	7
Colorimetric	Smartphone	10	10^1-10^7	90 min	8
Colorimetric	Smartphone	5.6	10^2-10^7	30 min	this work

References

1. X. Song, H. Wang, X. Shao and X. Xu, *Microchem J.*, 2024, **207**, 112111.
2. Y. Huang, Y. Zhang, X. Yan, Y. Zhao, M. Duan, X. Li and F. Jia, *Food Biosci.*, 2025, **63**, 105606.
3. R. Guo, L. Xue, G. Cai, W. Qi, Y. Liu and J. Lin, *ACS Appl. Nano Mater.*, 2021, **4**, 5115-5122.
4. Y. He, F. Jia, Y. Sun, W. Fang, Y. Li, J. Chen and Y. Fu, *Sens. Actuator B-Chem.*, 2022, **369**, 132301.
5. J. Zhuang, Z. Zhao, K. Lian, L. Yin, J. Wang, S. Man, G. Liu and L. Ma, *Biosens. Bioelectron.*, 2022, **207**, 114167.
6. L. Wang, T. Liao, H. Zhou, Y. Huang, P. Chen, X. Yang and X. Chen, *Anal. Biochem.*, 2021, **615**, 114068.
7. L. Xue, N. Jin, R. Guo, S. Wang, W. Qi, Y. Liu, Y. Li and J. Lin, *ACS Sens.*, 2021, **6**, 2883-2892.
8. Z. Su, S. Wei, X. Shi, X. Wang, L. Zhang, X. Bu, H. Xu, Y. Liu, M. Jin, B. Pang and C. Zhao, *Anal. Chim. Acta*, 2023, **1239**, 340672.